

The effect of the annealing temperature on the local distortion of $\text{La}_{0.67}\text{Ca}_{0.33}\text{MnO}_3$ thin films

Daliang Cao,^{a*} Frank Bridges,^a Corwin Booth^b and Daniel Worledge^c

^aPhysics Department, University of California, Santa Cruz, CA 95064, ^bLos Alamos National Laboratory, Los Alamos, NM 87545, and ^cDepartment of Applied Physics, Stanford University, Stanford, California 94305-4090. E-mail: dcao@maxwell.ucsc.edu

The colossal magnetoresistance (MR) of the $\text{La}_{1-x}\text{Ca}_x\text{MnO}_3$ system has been studied extensively. From our previous studies, we find there is an important connection between local distortions and magnetism in these materials. Recently, we have carried out Mn *K*-edge fluorescence experiments with thin film samples (3000 Å) of $\text{La}_{0.67}\text{Ca}_{0.33}\text{MnO}_3$: one is as-deposited; another one is post-annealed at 1200 K. We find that the local distortion decreases with increasing the annealing temperature. For measurements as a function of temperature, the change of the local distortion is largest for the 1200 K annealed sample. The small change for the as-deposited sample, which has the highest MR, indicates that another mechanism contributes.

Keywords: XAFS, thin film, CMR.

1. Introduction

The Double Exchange mechanism was originally considered to be the main interaction contributing to the colossal magnetoresistance (CMR) (Zener, 1951; Anderson & Hasegawa, 1955; de Gennes, 1960). Millis *et al.* suggested that local distortions also play an important role in CMR materials, and are needed to explain the large magnitude of the MR (Millis *et al.*, 1995). Several experiments have been done on powder samples of calcium substituted LaMnO_3 and an important relationship between local distortion and magnetism in the material has been found (Booth *et al.*, 1998*a,b*). The new experiments investigate the local structure of thin films of $\text{La}_{0.67}\text{Ca}_{0.33}\text{MnO}_3$ on SrTiO_3 substrates to understand more about this relationship. Transport measurements show that the annealing temperature affects the resistivity of these thin films very much. They also show that a huge MR occurs for the films, especially for the as-deposited sample.

2. Samples and experiments

2.1. Samples

The $\text{La}_{0.67}\text{Ca}_{0.33}\text{MnO}_3$ thin-film samples were made by D. C. Worledge using PLD; each film is 3000 Å thick. See Worledge *et al.* (1998) for additional details. The samples we chose for the XAFS were: as-deposited (750 K) and annealed at 1200 K. All samples have broad transitions and T_c increases with the annealing temperature. The as-deposited

sample shows a high resistivity compared with the other sample. Also, the magnetoresistance is very large for the as-deposited sample at very low temperature.

2.2. Experiments

The experiment was done on beamline 10-2 at SSRL using Si <220> monochromator crystals. We used the 13-element Ge detector to collect the Mn *K*-edge fluorescence data. The thin film samples were aligned at $\sim 55.0^\circ$ with respect to the X-ray beam to make x, y and z axes equivalent, and thus correspond to a powder. This angle comes from the polarization dependence of the photoelectric effect (Pettifer *et al.*, 1990). For each sample, we made four sweeps at each temperature, and for two of these sweeps, we rotated the sample by 1.5° in order to find out the position of glitches. Fig. 1 indicates the quality of the data.

3. Data and analysis

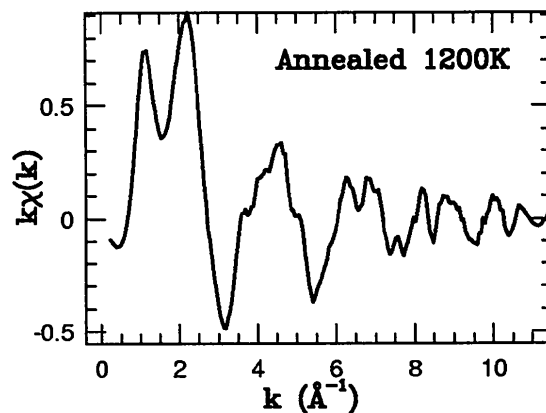


Figure 1

A plot of *k*-space data for the 1200 K annealed sample at 20 K to show the quality of the data

In Fig. 2, we show the Mn *K*-edge Fourier transformed (FT) *r*-space data for the two thin-film samples. We obtain some obvious results from this figure immediately. First, the amplitude of the Mn—O peak (the first peak) decreases with temperature. That means there are more distortions in each sample when the temperature is higher. Second, for the higher annealing temperature, the change of the amplitude with temperature for the Mn—O peak is larger; most of the disorder is removed for the 1200 K annealed sample when the temperature decreases to 20 K. In contrast, most of the distortion in the as-deposited sample still remains at $T = 20$ K.

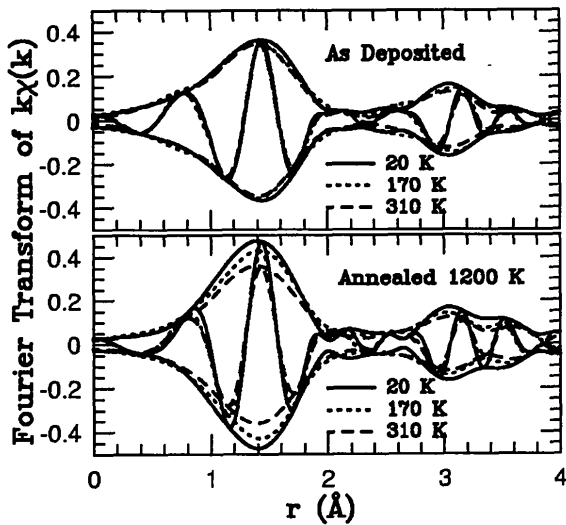


Figure 2

A comparison of the change in r -space data with temperature for the $\text{La}_{0.67}\text{Ca}_{0.33}\text{MnO}_3$ thin-film samples with different annealing temperature. Top one is 750 K annealed (as deposited), bottom one is 1200 K annealed. FT range is $3.3\text{--}10.5 \text{ \AA}^{-1}$, with 0.3 \AA^{-1} Gaussian broadening.

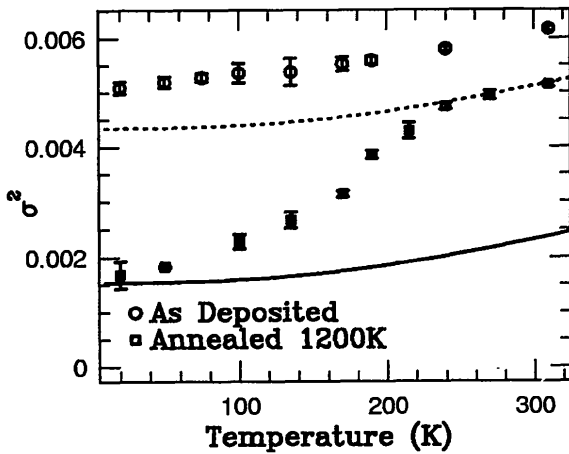


Figure 3

A plot of σ^2 vs temperature for the as-deposited and 1200 K annealed $\text{La}_{0.67}\text{Ca}_{0.33}\text{MnO}_3$ thin-film samples. (Here σ is the width of the first peak (Mn—O peak) in the r -space graph.) The solid line is the thermal contribution σ_T^2 , and the dotted line is $\sigma_T^2 + \sigma_{FP}^2$ for the annealed 1200 K sample.

Detailed fits to the data were carried out using FEFF6 theoretical functions (Zabinsky *et al.*, 1995). In the fit, S^2N (N is the number of nearest neighbours) was set at 4.3 and the pair-distribution width, $\sigma(T)$, was determined. In Fig. 3, we plot σ^2 vs temperature. For the as-deposited sample, σ^2 has a very small change with decreasing temperature, while for the 1200 K annealed sample, the change in σ^2 is large. We also find in Fig. 3 that, at high temperatures, σ^2 is larger for the as-deposited sample at all temperatures. This indicates that some distortion has been removed in the annealing process.

The solid line in Fig. 3 correspond to the data for CaMnO_3 , which has a large Debye temperature; σ^2 for this sample will be denoted σ_T^2 . If this curve is shifted vertically, corresponding to a static disorder contribution, σ_{FP}^2 , the same curve fits the high temperature data (above $T=240 \text{ K}$). The excess broadening, $\Delta\sigma^2(T)$, which is associated with the formation of polarons, is the difference between the dotted line and the data for the 1200 K annealed sample. A similar analysis is carried out for the as deposited sample. In Fig. 3 we only show $\sigma_T^2 + \sigma_{FP}^2$ for the 1200 K annealed sample as an example. The maximum difference obtained at the lowest temperature is considered to be the fully-developed polaron distortion, σ_{FP}^2 . In Fig. 4, we plot $\ln \Delta\sigma^2$ vs M/M_0 , where $\Delta\sigma^2$ is given by:

$$\Delta\sigma^2 = \sigma_T^2 + \sigma_{FP}^2 - \sigma_{\text{Mn-O}}^2$$

A previous study of $\text{La}_{1-x}\text{Ca}_x\text{MnO}_3$ powder samples showed that there is a linear relationship between $\ln \Delta\sigma^2$ and the magnetization (Booth *et al.*, 1998a,b), which provides evidence that there is a strong connection between local distortion and magnetism in these materials. From Fig. 4, there is a similar connection between local distortions and magnetism; it is still a straight line for the as-deposited sample, but for the 1200 K annealed sample, we find an obvious deviation from the straight line. The data appear to lie on two different straight lines. That may indicate that there are other mechanisms involved for the thin-film samples.

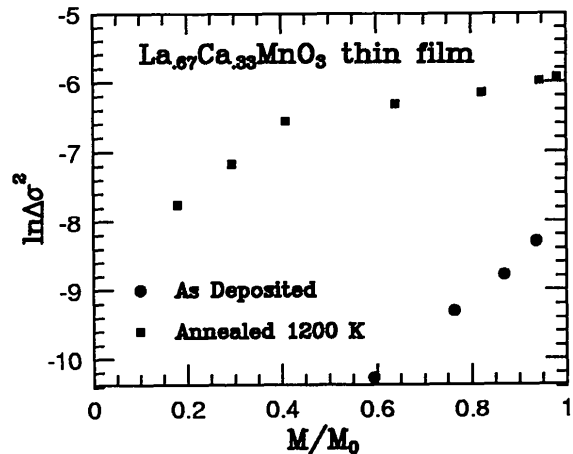


Figure 4

A plot of $\ln \Delta\sigma^2$ vs M/M_0 for the as-deposited and 1200 K annealed $\text{La}_{0.67}\text{Ca}_{0.33}\text{MnO}_3$ thin-film samples. M is the measured magnetization and M_0 is the magnetization at the lowest measuring temperature; M/M_0 is the relative magnetization.

4. Conclusion

From our analysis, we find that the annealing temperature of the thin film affects the local distortion of the materials appreciably. The large change in resistivity and the small change in local structure with temperature for the as-deposited sample suggest that only small regions are contributing to the resistivity and percolation may play a role.

We also find that there is still a strong connection between local distortions, resistivity and the magnetism in the thin-film materials, but other mechanisms may also be important in this case.

5. Acknowledgement

This work was supported in part by NSF grant DMR9705117. The experiments were performed at SSRL, which is operated by the DOE, Division of Chemical Sciences, and by the NIH, Biomedical Resource Technology Program, Division of Research Resources. Some experiments were carried out on UC/National Laboratories PRT beam time.

References

- Anderson, P. W. & Hasegawa, H. (1955). *Phys. Rev.* **100**, 675-681.
- Booth, C. H., Bridges, F., Kwei, G. H., Lawrence, J. M., Cornelius, A. L. & Neumeier, J. J. (1998). *Phys. Rev. Lett.* **80**, 853-856.
- Booth, C. H., Bridges, F., Kwei, G. H., Lawrence, J. M., Cornelius, A. L. & Neumeier, J. J. (1998). *Phys. Rev. B* **57**, 10440-10454.
- de Gennes, P. G. (1960). *Phys. Rev.* **118**, 141-154.
- Millis, A. J., Littlewood, P. B. & Shraiman, B. I. (1995). *Phys. Rev. Lett.* **74**, 5144-5147.
- Pettifer, R. F., Brouder, C., Benfatto, M., Natoli, C. R., Hermes, C., & Ruiz Lopez, M. F. (1990). *Phys. Rev. B* **42**, 37-42.
- Worledge, D. C., Mieville, L. & Geballe, T. H. (1998). *J. Appl. Phys.* **83**, 5913-5916.
- Zabinsky, S. I., Ankudinov, A., Rehr, J. J. & Albers, R. C. (1995). *Phys. Rev. B* **52**, 2995-3009.
- Zener, C. (1951). *Phys. Rev.* **82**, 403-405.

(Received 10 August 1998; accepted 18 January 1999)